UNIVERSITY OF CALIFORNIA
RIVERSIDE

Morphological Analysis of C57Bl/6 Murine Hippocampal Iba-1^{+} Microglia In Response to *Alternaria alternata*

A Thesis submitted in partial satisfaction
of the requirements for the degree of

Master of Science

in

Biomedical Sciences

by

Taher Bhaijee

June 2022

Thesis Committee:
Dr. Monica Carson, Chairperson
Dr. Marcus Kaul
Dr. Iryna Ethell

The Thesis of Taher Bhaijee is approved:

_____

_____

_____

Committee Chairperson

University of California, Riverside

Acknowledgements

Thank you to my wife, Fiona Bhaijee, for loving and supporting me throughout this entire journey. Thank you to my mentor, Dr. Monica Carson, for all the support that she is given me through these past few years. Thank you to my dissertation committee, Dr. Ethell and Dr. Kaul, for teaching, helping and guiding me during medical school and graduate school classes. Thank you to the Carson lab graduate and undergraduate students without whom this would not be possible. Thank you to my parents, Feroze and Tasneem Bhaijee, for supporting me and believing in me. Finally, I would like to dedicate this to my daughters, Rumi Bhaijee, my sunshine and Luna Bhaijee, my moonshine.

ABSTRACT OF THE THESIS

Morphological Analysis of C57Bl/6 Murine Hippocampal Iba-1^{+} Microglia In Response to *Alternaria alternata*

by

Taher Bhaijee

Master of Science, Graduate Program in Biomedical Sciences
University of California, Riverside, June 2022
Dr. Monica Carson, Chairperson

Microglial morphology is difficult to quantify. Currently, there are no agreed upon systemic method of quantification of microglial morphology within the healthy brain or in response to an injury. Studies have proposed myriad models of morphological changes in microglial reactivation and recent studies have found sex differences in microglia. To examine changes in the microglia of murine hippocampus, we immunofluorescent identified microglia, in coronally sectioned tissues, using ionized calcium-binding adapter molecule-1 (Iba-1) labeling. We used three methods to examine microglia morphology: mean fluorescence intensity, soma volume, and single-cell tracing. For soma volume and single cell tracing, we reconstructed the 3D microglia in the Neurolucida software and analyzed their morphology using Sholl analysis. We used *Alternaria alternata* in our environmental chamber to model peripheral allergic inflammation. We found that female microglia increase their cell number and nodes while males did not. We conclude that females are more responsive to *Alternaria* than males, increasing their cell density and surveillance.

Table of Contents:

List of Figures

Introduction:

Functions of Microglia at Homeostasis:

Microglia, the resident immune cell in the central nervous system (CNS), perform essential roles in brain function and brain development under homeostatic conditions. However, microglia exhibit widely differing functions depending on the stage of life, sex, CNS region, and context of health or disease. Differences in microglial number, morphology, and gene expression have been reported between these contexts. (Lawson et al., 1990) As a result, the term "homeostatic microglia" needs context. In this data set, the context for "homeostatic microglia" means adult C57Bl/6 mice, aged 2-3 months (P60-90) or pup, aged 2 weeks (P15), male or female, hippocampus or brainstem or olfactory bulb, and in the context of the UCR Vivarium or 1 week exposure to *Alternaria alternata.* If the homeostatic microglia have another context, then the term will not be used, and the context will be specified (For example, microglia from rats or humans in the hippocampus in response to LPS.) (Paolicelli et al, 2022).

One of the most important tasks of homeostatic microglia is surveillance. Surveillant activities include synaptic pruning, monitoring neuronal function, and scavenging for cellular debris and tissue repair. Studies have shown that microglia reside in specialized states (Hammond et al., 2019a). In a homeostatic adult hippocampal mouse, microglia adopt a ramified morphology characterized by a small cellular body ranging from 100 -200 μm^3 and multiple 3-5 long thin branched processes that can extend up to 50-60 μm (Smolders et al., 2019). The studies of Nimmerjahn and Davalos observed that homeostatic microglial processes are motile in the absence of

immunological activity, regularly extending and retracting their processes ((Davalos et al., 2005; Nimmerjahn et al., 2004). Homeostatic microglial processes make direct contact with neuronal synapses once per hour, responding to neuronal activity and regulating synaptic connectivity(Wake et al., 2009). These microglia will respond to changes to their microenvironment. Microglia using purinergic receptors will respond to ATP, changing their morphology and directing their processes towards the site of injury (Davalos et al., 2005). Under anesthesia, homeostatic human microglia in the somatosensory cortex were found to increase their surveillance activity by extending their processes using adrenergic not purinergic receptors (Liu et al., 2019). Homoeostatic microglia, in the adult rat in the prefrontal cortex, have been shown to exhibit consistent morphology across all layers from medial to lateral (Kongsui et al., 2014). The microglia are an extremely plastic cell that can change its function and its morphology depending on the context including brain region, sex, age and in response to insults or exposures.

Heterogeneity of Microglia at Homeostasis

Are microglia a heterogenetic population? Depending on the brain region, Lawson was the first to describe clear regional differences in microglial morphology. He described the occurrence of compact (round, short processes), longitudinally branched (long primary processes) and radially branched (tortuous processes with secondary branching) microglia. Radially branched microglia are typically found in gray matter tracts such as the hippocampus while longitudinally branched microglia are typically found in white matter tracts such can be found in the brainstem. (Lawson et al., 1990) With the advent of single-cell RNA sequencing (RNAseq), microglia populations have

been clustered and subclustered in various ways. The microglia can now be grouped into distinct subtypes, but the degree of transcriptome and proteome heterogeneity that is sufficient for defining cell subtypes is currently under debate. A study by Hammond et al., found 9 transcriptionally distinct microglia states, which expressed unique sets of genes and were localized in the brain using specific makers. (Hammond et al., 2019b). Another study by Li et al. found 14 distinct microglia states. (Li et al., 2019). After these numerous RNAseq data sets were published, Masuda challenged the idea of heterogeneity of adult microglia and instead proposed context-dependent heterogeneity of homeostatic microglia. For example, CNS associated macrophages (CAM) used to be a part of the microglia population but can now be categorized as a distinct cell population with a different transcriptional signature than traditional microglia. (Masuda et al., 2020) Furthermore, it is currently being studied and debated what homeostatic microglia would look like versus disease-associated microglia (DAM). The main idea is that microglia are still a heterogenous population, but we can now redefine some of the clusters of microglia and thereby remove some of the heterogeneity by subpopulating or subtyping the microglia.

Development of Sexually Dimorphic Adult Microglia at Homeostasis

Recent fate mapping studies have shown that microglia originate from a pool of RUNX-postive, Myb-independent macrophages produced during primitive hematopoiesis in the yolk sac, which start invading the neuroepithelium from E8.5 in mice (Ginhoux et al., 2009). As a result, microglia are the only cell in the brain not originating from ectoderm. On arriving, the cells possess a round cell body with no identifiable processes

(Mizutani et al., 2012). The cells migrate to their home destination when microglial process extension starts. At postnatal day 20 (P20) no sex-related difference in Iba^+ cell numbers were identified but by postnatal day 30 (P30), microglial numbers were increased in the hippocampus of female rats(Schwarz et al., 2012). By postnatal day 60 (P60), microglia had developed processes but sex-related difference in morphology was noticed where the females had thicker and longer processes. By P60, males had greater phagocytic function, greater expression of MCH Class II, CD 68 and Triggering Receptor Expressed on Myeloid cells (TREM2) (Guneykaya et al., 2018). As a result, recent studies have hypothesized that homeostatic microglia are sexually dimorphic during development and continue their differences into the adult homeostatic microglia.

Studies have reported sex differences in transcriptomic, proteomic, density and morphology of the male and female homeostatic adult microglia in the hippocampus and cortex. In pup and adult male microglia, microglia density was increased in the hippocampus. However, soma size was increased in the hippocampus of female adults, but not female pups. The soma size of pup male and female were the same (Guneykaya et al., 2018). Transcriptome data found several hundred genes that were differently expressed by sex in the cervical spinal microglia. These differently expressed genes (DEGs) included upregulated genes involved with proinflammatory cytokine viral infection and regulation of RNA transcription while the downregulated genes involved pathways including oxidative pathways (Ewald et al., 2020). Our lab found similar results in the olfactory bulb and brainstem (Valdez, 2021). Another study found that in their RNA-seq analyses female microglia express genes involved in cell plasticity, the control

of the inflammatory response and repair mechanisms. Female microglia had increased production of tumor necrosis factor (TNF) and interleukin -1 beta (IL-1β). Microglia from the cortex, spinal cord, hippocampus, and olfactory bulb show subtle differences in gene expression levels compared to microglia in the cerebellum and eyes (Villa et al., 2018). In conclusion in a healthy mouse, we already see sex differences in microglia before they respond to an insult.

Reactive Microglia in response to infectious peripheral inflammation, the LPS model

Peripheral immune cells can cross the intact blood brain barrier and reach CNS neurons and glia actively regulate macrophage and lymphocyte responses. Microglia are immunocompetent but differ from other macrophage cells in their ability to direct neuroprotective lymphocyte responses(Carson et al., 2006). A model of bacterial peripheral inflammation has been well described where lipopolysaccide (LPS), an endotoxin found on gram-negative bacteria, can be injected intraperitoneally in the mouse to mimic a systemic inflammation. The immune response to LPS is the classical pathway which involves LPS binding to Toll-like receptors 2 and 4 (TLR2, TLR4) in dendritic cells which upregulate nuclear factor kappa B (NF-κB) and releasing pro-inflammatory cytokines and chemokines such as interferon gamma (INFγ), interleukin-1beta (IL-1β), and interleukin -6 (IL-6). Systemic increases in these chemokines in the blood lead to changes in the neuroimmune state from interactions of the cytokines in the brain vasculature or the interaction with peripheral nerves sensing the peripheral inflammation. The peripheral inflammation leads to microglial reactivation within 24 hours. The microglia stay activated for at least 48 hours and return to their normal state within 28

days(Qin et al., 2007). In microglial reactivation in response to LPS, the gene expression for phagocytosis gets upregulated. Morphologically, the microglia retract their processes and become more ameboid-like. Around 7 days, the innate immune system promotes the adaptive immune system in the form of a T-helper cell type 1 (Th-1) response (Carson, 2012).

Reactive Microglia in response to allergic inflammation, the Alternaria model

A model of allergic inflammation was developed where mice were housed in a chamber thereby studying the health effects of aerosolized materials with restricting movement or feeding behavior. In the chamber, the mice can be exposed to fine or ultrafine particulates continuously for a certain period. Continuous exposure to *Alternaria alternata* for 96 hours induced pulmonary inflammation including neutrophils, eosinophils, and lymphocytes modeling an allergic inflammatory response (Peng et al., 2018). However, in the whole brain without the medulla, the overall basal level of innate immune molecules did not decrease, but the medulla did show a decrease of the innate immune molecules. This points to a brain-region specific effect. In addition, continuous exposure to *Alternaria alternata* decreases Iba-1 immunoreactivity suggesting that the hippocampal adult microglia are downregulating their genes around 4 days (Peng et al., 2018). Furthermore, subsequent gene expression data in our lab shows a downregulation of the activated microglia pathway at 5 days consistent with our morphological results. However, we also see an upregulation at 7 days in the microglia pathway (Valdez, 2021). Klein also reported a decrease in Iba-1 immunoreactivity but used a different method to induce allergic inflammation by injecting adjuvants multiple times (Klein et al., 2016).

Implications for Neurological Diseases

Many neurological diseases are marked by differences in their prevalence, incidence, symptoms, and progression between males and females. The reasons for these sex differences are not well understood. Studies have reported sex differences in neurodevelopmental diseases such as autism spectrum disorder (ASD) and attention deficit hyperactivity disorder (ADHD), neuropsychiatric diseases such as schizophrenia, depression, and anxiety, and neurodegenerative disorders such as Alzheimer's, Parkinson's disease, and frontotemporal dementia (Table 1). In Alzheimer's disease, the prevalence of the disease in individuals over 65 is 2-3 times greater in women than men. Hippocampal atrophy is worse and progresses more rapidly in women than men (Ardekani et al., 2016).

Table 1: Breakdown of Neurological Diseases which have sex differences

Neurodevelopmental Diseases	Neuropsychiatric Diseases	Neurodegenerative Diseases
Autism Spectrum Disorder (ASD)	Schizophrenia	Alzheimer's disease (AD)
Attention Deficit Hyperactivity Disorder (ADHD)	Depression	Parkinson's disease (PD)
	Anxiety	Frontotemporal dementia (FTD)

Some of the statistics on sex differences in diseases could be underdiagnosed in the clinic. Autism is often stated to have a sex difference. Nearly 4-3 times less females are diagnosed with autism than males. But autism in females is underdiagnosed. Most clinicians look for male-like autism symptoms in females and miss female-like autism symptoms in females. (Morgan et al., 2010) Microglia have been implicated in these

neurological diseases. (“2021 Alzheimer’s Disease Facts and Figures,” 2021; Bachstetter et al., 2015; Franco-Bocanegra et al., 2021; Ulrich et al., 2017). It has been theorized that dysfunctional microglia are thought to play a part in the pathogenesis of these diseases. Table 2 has compilation of sex differences in the diagnosis of these neurological diseases.

Table 2: Comparison of Sex Differences between Diseases

Disease	Sex Differences between Diseases
Alzheimer disease	Females are ~2.0 more likely to be diagnosed than males
Parkinson disease	Females are ~1.5-2.0 less likely to be diagnosed than males
Autism Spectrum Disorder	Females are ~4.0 less likely to be diagnosed than males
Schizophrenia	Females are ~ 1.4 less likely to be diagnosed than males
Multiple Sclerosis	Females are ~2.8 more likely to be diagnosed than males

Materials and Methods

Mice

Male C57BL/6J adults were maintained in standard mouse cages with fresh bedding and standard Purina food for the duration of each experimental exposure, unless otherwise stated. All experiments were performed in compliance with University of California Institutional Animal Care and Use Committee regulations and reviews.

Chamber Exposure

The environmental chamber being used was constructed by Dr. Xinze Peng in collaboration with Dr. David Lo and Dr. David Cocker. The chamber was constructed using clear acrylic sheets with internal dimensions of 40 x 32 x 25 in^3 (length x width x height; 540 L in volume). Two perforated aluminum plates separated the inlet and the outlet to enable uniform dispersion of injected aerosols. Attached to the top of the chamber is a LED warm light string to provide a 12:12 hour light:dark cycle. The whole chamber was covered with blackout cloth to ensure zero light contamination from outside. A $\frac{1}{4}$ in. inlet from the upper left of the chamber was used for injection while four $\frac{1}{2}$ in. exhaust ports located in the lower right chamber ensured that the in-chamber pressure remained the same as atmospheric. Another $\frac{1}{4}$ in. outlet located in the lower right of the chamber was used for instrument sampling and monitoring. The chamber was flushed with clean air with at least 10 chamber volumes before and after each test to avoid contamination.

The exposure chamber consists of three main portions. The first portion is where lab air is passed through multiple inline filters followed by a HEPA filter before it reaches the Alternaria liquid suspension (0.26 g/mL). The air/suspension mix is then atomized, dried and delivered into the chamber. The second portion is the chamber is constructed from plexiglass, with a LED light attached to the top with a timer to maintain the 12:12 day:night cycle. Two porous aluminum plates are used to allow for full dispersion of the aerosolized extract across the chamber. The third portion is the multiple detectors continuously measure aspects of the aerosol such as its concentration, size (diameter), and distribution throughout the chamber. The level of ammonia is monitored to prevent toxic build up from excrements in the cage. (Peng et al., 2018; Valdez, 2021)

Alternaria Extract

Alternaria alternata is a common fungus found in soil of desert climates. It can produce many spores which make exposure to the allergen inevitable in both indoor and outdoor environments. *Alternaria* has also be shown to increase the severity of pre-existing inflammatory conditions such as asthma or allergic rhinitis. For our experiments we will suspend our *Alternaria* extract in ultrapure water where it will be atomized and distributed within the chamber at an average amount of 1100-1400 ug/m^3. (Peng et al., 2018; Valdez, 2021)

Brain Dissections, Immunofluorescent (IF) Staining, and Imaging

The mice were transcardially perfused with 20 mL of PBS and then 20mL of 4% PFA. Whole brains were then dissected and immediately submerged in 4% PFA for 24hr at 4°C, followed by 48hr in 4% PFA/30% sucrose solution. Coronal sections of

hippocampal regions were cryosection (25 μm). Hippocampal sections were stored in one of 8 collection tubes containing CBS cryopreserving solution and then stored at -80°C. Tissue was placed onto Fischer Superfrost plus slides and exposed to rabbit anti-Iba1 antibodies (Wako), followed by incubation with Alex-680 conjugated goat anti-rabbit. Tissue sections were mounted in Prolong Gold containing DAPI and subsequently imaged on a Yokogawa spinning disc confocal microscopy system. Hippocampal tissue was imaged on a Yokogawa spinning disc confocal microscopy system along the stratum radiatum of the CA1 region in the dorsal hippocampus. Each animal had 3 consecutive 20X z-stacked images taken (25 optical slices, 1.19 μm thickness). Max projections of these images were then split into quadrants and one microglial cell from 3/4 quadrants were then further imaged at 63X (45 optical slices, 0.37 μm thickness).

Mean Fluorescence Intensity

Immunofluorescence was quantified with NIH Image J (version 1.5K) using the Mean Gray Value tool (sum of the gray values of all pixels in specific fluorescent channel divided by the number of pixels in the specific fluorescent channel in the total image). The images were split into their separate channels and the green channel (Iba-1) was measured for mean gray value. Each z-stack was measured and averaged for each tissue. Each tissue was averaged for each biological sample.

Cell Soma Body Analysis

Cell Soma bodies were analyzed using Neurolucida software. The images were split into their separate channels using FIJI and the green (Iba-1) was loaded into the Neurolucida software (2018.1.1). The images were initially scaled (*single voxel = 0.279877 x*

0.279877 x 1.19 µm). The soma body was detected and traced by utilizing size parameters (Size Constraint = 2; Interactive Search Region = 13; and Soma Detector Sensitivity = 75 ± 10%). The Soma body tracing was saved and opened using Neurolucida Explorer. Cell body volume and surface area was collected for each image in Neurolucida Explorer using Analyze>Structure>Branched Structure Analysis>Cell Body.

Sholl Analysis

Microglia morphology was measured using Neurolucida software. The images were then split into their separate channels using FIJI and the green channel (Iba-1) was loaded into Neurolucida software (2018.1.1). The images were initially scaled (*single voxel = 0.087819 x 0.087819 x 0.037 µm*). The soma was detected by utilizing size parameters (Size Constraint = 2; Interactive Search Region = 13; and Soma Detector Sensitivity = 75 ± 10%). Automatic user-guided tracing which utilizes a sampling technique known as Scooping Voxel (Typical Process Width = 1.41 µm) was used since it is good for images with high contract between the cells and the background (Sensitivity = 70; Gap Tolerance = 0.70 µm). The software then places seeds, guides for tracing, along the extensive processes of each cell (Dense; Sensitivity = 90%). By allowing for the detection of axial edges, edges perpendicular to the axis of rotation, and allowing for tracing with super-ellipsoids (wit = 20; iterations = Always; Size Range in Pixels: Min 10, Max 18) volumetric measurements from each microglial process was able to be collected. For a process to be considered part of the cell being measured, it had to be within 2 µm of the main process, have a max angle of deviation of 79°, and a min ratio of 22% (the leeway given to adjust the process length). The resulting trace was then inspected for superfluous

seeds/processes and brought into the 3D environment. Microglia were then analyzed with Neurolucida Explorer Sholl Analysis (Starting Radius = 10 μm; Radius Increments = 5 μm) (Okeke, 2021).

Statistics

Values are reported as means with standard error of the mean (SEM), with sample size reported in each assay. Unpaired Student's t-test were used to analyze MFI, Cell Count and Soma Volume. Two-way analysis of variance (ANOVA) with post-hoc Tukey's multiple comparison test were used to analyze Sholl data indicated using Prism9 (Graphpad Software, La Jolla, CA). In all data sets, alpha is equal to 0.05.

Results

Microglia did not change their Iba-1 immunoreactivity and their soma volume in response to 7-day exposure to *Alternaria,* but female microglia increased their cell numbers.

Previous experiments showed that hippocampal adult microglia showed a decrease in Iba-1 immunoreactivity in response to 96-hour exposure to *Alternaria*. We hypothesized that microglia would have a similar decrease in Iba-1 immunoreactivity, but our results show that they stay the same. This is consistent with the gene expression data that we collected at 5 day and 7-day time points. We hypothesize that they return to their baseline immunofluorescence at 7 days. At 7 days, the innate immune system is at its peak and it is changing to an adaptive immune response. Hippocampal male adult microglia, hippocampal female adult microglia, hippocampal male pup microglia and hippocampal female pup microglia did not have a significant change in mean fluorescence intensity and thus did not have a significant change in Iba-1 immunoreactivity. Hippocampal male adult microglia, hippocampal female adult microglia, hippocampal male pup microglia and hippocampal female pup microglia did not show a change in soma volume and thus did not have an obvious reactivation as shown in LPS or traumatic brain injury (TBI) studies. Previous data in our lab has shown that an increase in soma volume in the male adult olfactory bulb (Valdez, 2021). However in the hippocampus, this effect is not present. Hippocampal female adult microglia and hippocampal female pup microglia did show an increase in cell count while hippocampal male adult microglia and hippocampal male pup microglia did not show a significant increase. In fact, they show a decrease in

cell count. This could indicate that the female microglia are increasing their cell density or proliferating in response to 7 day exposure to *Alternaria*. After calculating the soma volume, we noticed that there was no difference in the average of somal volume. However, we wanted to see if there was a difference in the variance of somal volume. We did not see a difference in the somal volume between mice nor between conditions.

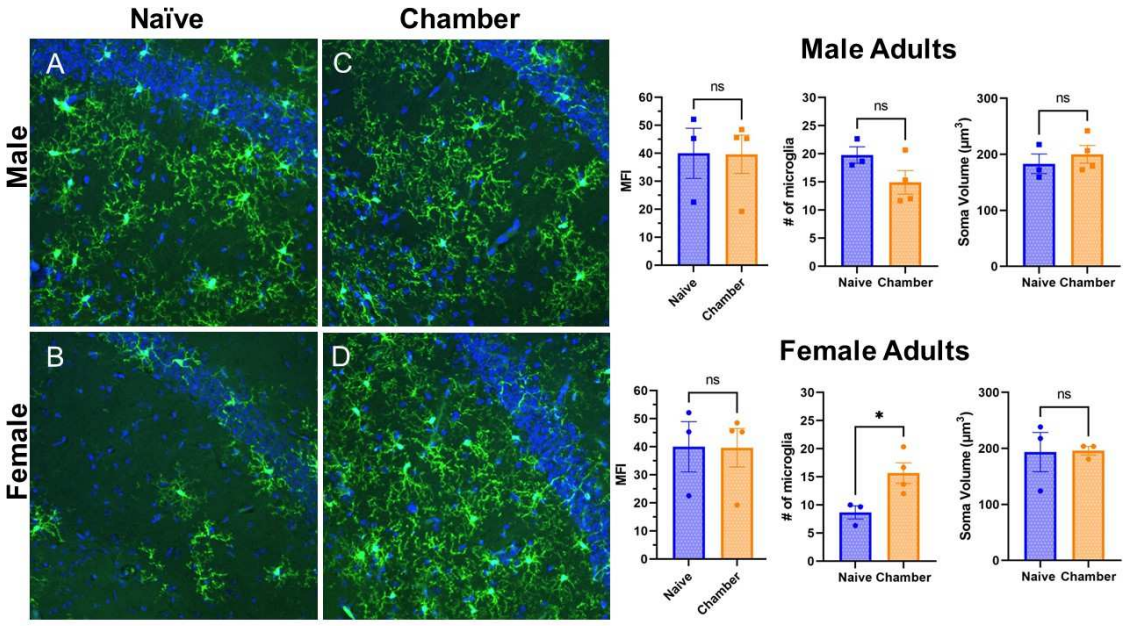

Figure 1: Sex differences in Adult Mice.
The images (A-D) are IF stained with Iba-1 of CA1 of Hippocampus at 20X. (A) is Naïve Adult Male (N = 3 biological sample, n = 3 tissue samples), (B) is Naïve Adult Female (N = 3 biological sample, n = 3 tissue samples), (C) is Chamber Adult Male (N = 4 biological sample, n = 3 tissue samples), (D) is Chamber Adult Female (N = 4 biological sample, n = 3 tissue samples). MFI, cell count and soma volume were calculated for the images. For male MFI, p=0.9770, for female MFI, p=0.8531, for male cell count, p=0.1379, for female cell count, p = 0.0321*, for male soma volume, p=0.5064. for female soma volume, p=0.9445.

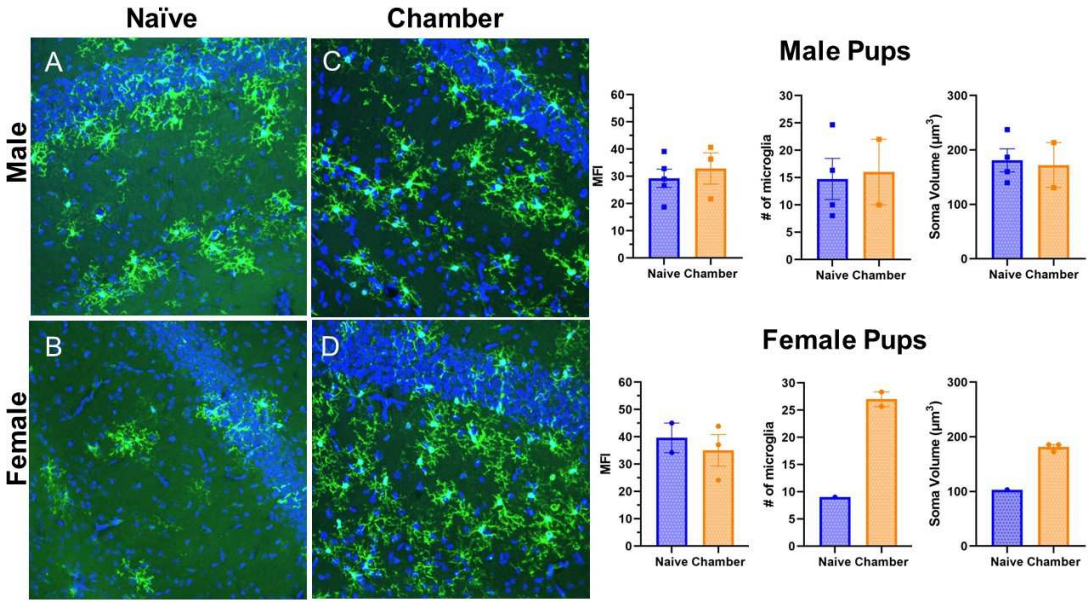

Figure 2: Sex Differences in Pup Mice
The images (A-D) are IF stained with Iba-1 of CA1 of Hippocampus at 20X. (A) is Naïve Pup Male (N = 3 biological sample, n = 3 tissue samples) (B) is Naïve Pup Female (N = 1 biological sample, n = 3 tissue samples) (C) is Chamber Pup Male (N = 2 biological sample, n = 3 tissue samples) (D) is Chamber Pup Female (N = 2 biological sample, n = 3 tissue samples). MFI, cell count and soma volume were calculated for the images. Statistical analysis not calculated due to incomplete data set.

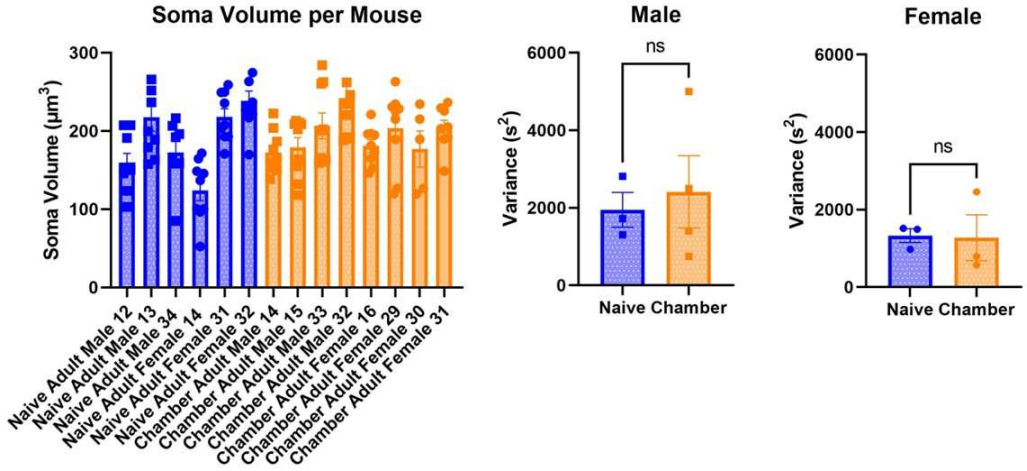

Figure 3: Variance of Soma Bodies
The average and variance of the soma bodies between mice and between condition. In the males, p = 0.707 and in the females, p = 0.934.

Microglia did not change their number of intersections, total length, surface area, volume, and average diameter in response to 7-day exposure to *Alternaria,* but female microglia increased their nodes.

We hypothesized that microglia were having subtle changes to their morphology after exposure to *Alternaria* due to qualitive analysis of the immunofluorescence images. We developed a method to quantitatively analyze the microglia by 3D single cell tracing. Then we used Sholl analysis to measure the number of intersections, nodes, total length, surface area, volume, and average diameter of the microglia. Hippocampal male adult microglia did not have a statistically significant change in the number of intersections, nodes, total length, surface area, volume, and average diameter in response to 7-day exposure to *Alternaria.* Hippocampal female adult microglia did not have a statistically significant change in the number of intersections, total length, surface area, volume, and average diameter in response to 7-day exposure to *Alternaria.* Hippocampal female adult microglia had a statistically significant change in the number of nodes. This could indicate that the female hippocampal adult microglia show increased surveillance capacity in response to a 7-day continuous exposure to Alternaria.

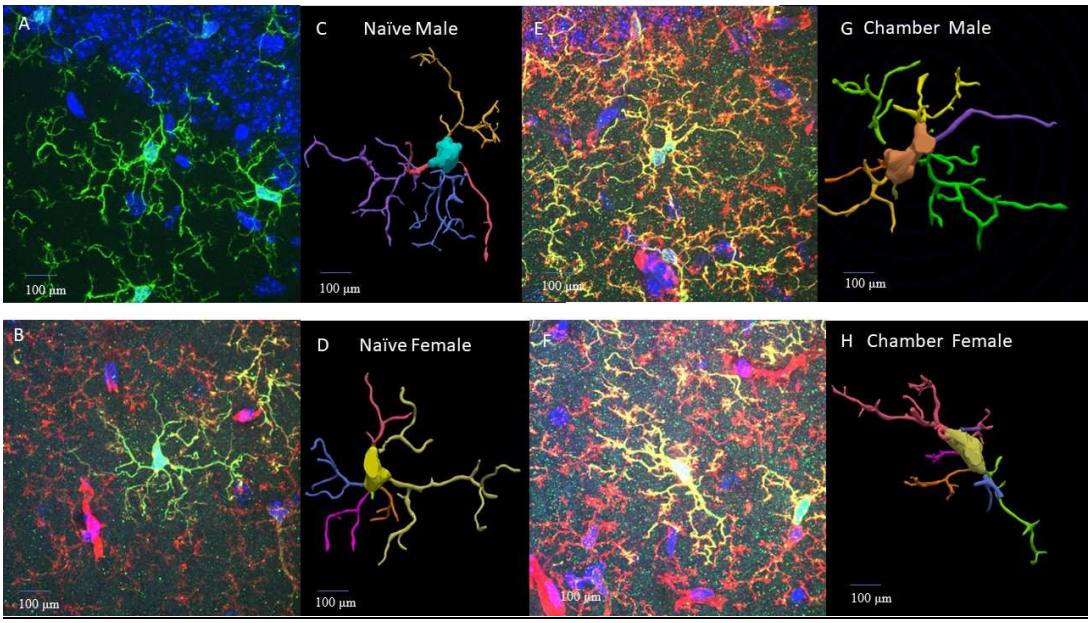

Figure 4: Tracing of Hippocampal Murine Adult Microglia at 63X.
(A) Max projection of z-stack of naïve male (B) Max projection of z-stack of naïve female (C) Neurolucida tracing of naïve male (D) Neurolucida tracing of naïve female (E) Max projection of z-stack of chamber male (F) Max projection of z-stack of chamber female (G) Neurolucida tracing of chamber male (H) Neurolucida tracing of chamber female

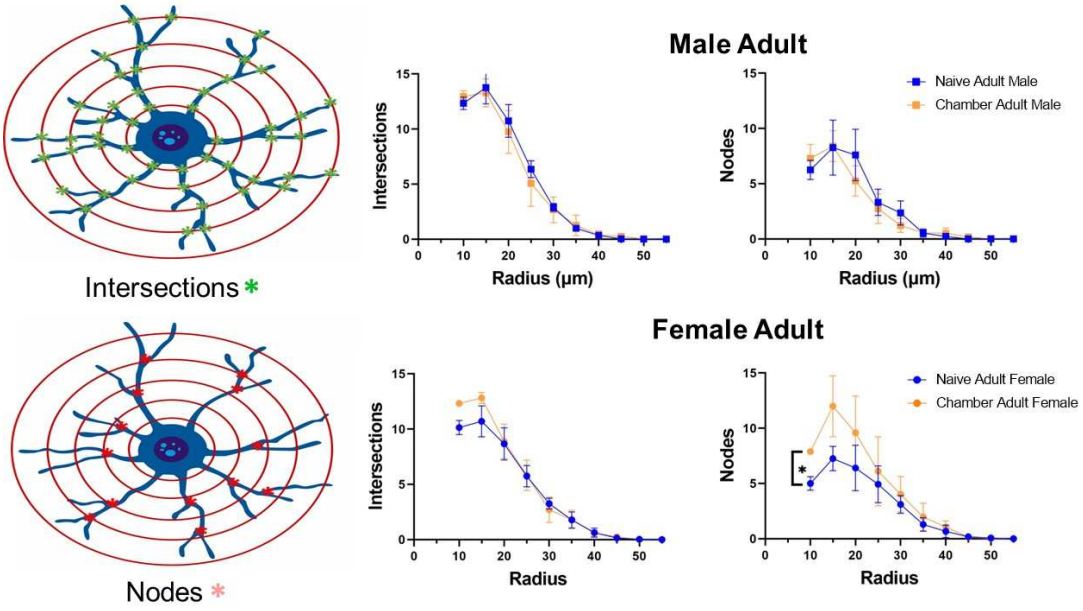

Figure 5: Intersections and nodes hippocampal murine adult microglia continuously exposed to *Alternaria Alternata* for 7 days. N = 3 naïve mice and 4 chamber mice (biological samples), n = 9 microglia per mouse. For female nodes, p = .0399.

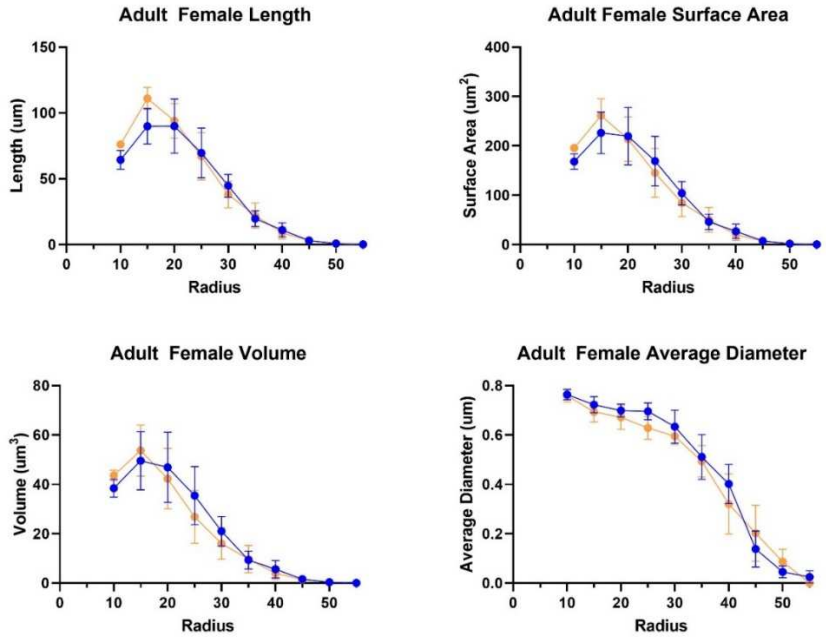

Figure 6: Length, surface area, volume, and average diameter of female hippocampal murine adult microglia exposed to *Alternaria Alternata* for 7 days. N = 3 naïve mice and 4 chamber mice (biological samples), n = 9 microglia per mouse.

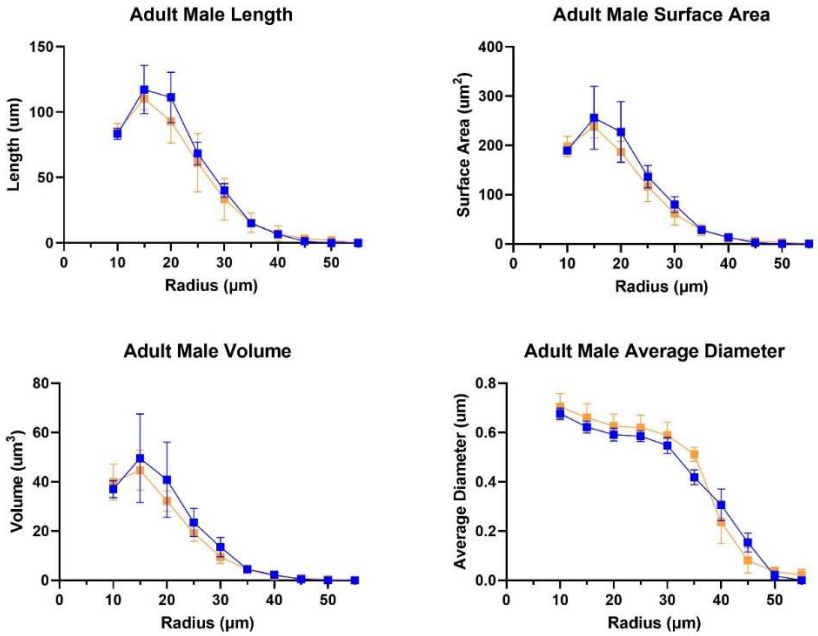

Figure 7: Length, surface area, volume, and average diameter of male hippocampal murine adult microglia exposed to *Alternaria Alternata* for 7 days. N = 3 naïve mice and 4 chamber mice (biological samples), n = 9 microglia per mouse.

Discussion:

The chamber exposure model is an innovative way of studying the effect of allergic peripheral lung inflammation on the microglia. We expose the mice continuously for 7 days to *Alternaria* extract particulates which induces a significant increase in neutrophils, eosinophils, and T-cell lymphocytes in the lung (Peng et al., 2018). In this model, the mice can freely move around their cage instead of being restrained to induce the allergen with ovalbumin or another adjuvant. Then we were able to image the microglia in the hippocampus and reconstruct them to see morphological changes. We found that the microglia only have slight changes. Our lab hypothesizes that the microglia become "bushier" when responding to allergic lung inflammation. However, "bushier" is a very subjective term, so we developed methods to quantitatively measure the morphology of the microglia.

Morphometric approaches keep evolving to overcome the multiple difficulties encountered when trying to extract accurate quantitative data from such a complex structure with a reasonable efficiency. A common approach for quantitative analysis of images of immunofluorescent labelled material is a technique called thresholding. An image is acquired on a confocal microscope and then processed with an analysis program (FIJI, or others). A particular pixel intensity level (the threshold) is manually defined and then used to determine what is "signal" (Iba-1) and "noise" (non-specific material attributable to the immunolabelling process). The number of pixels within a signal range is then quantified and compared across treatment groups. Instead of defining a threshold, we can also take the mean of the pixel intensity level. This process only works if the

same primary and secondary antibodies are applied to all tissues, the same reagents should be used at the same concentrations, and all incubation and development times should be identical. (Johnson & Walker, 2015) An alternative form of this technique is to take the average of all the immunofluorescent signal instead of setting a threshold. This technique is the mean fluorescence index (MFI). Again, this method can result in high variability if different staining or imaging protocols are used. Also, microglia have different cell density and different cell proliferation rates depending on the brain region which could shew results. An extension of this technique is to use cumulative thresholding spectra (CTS) which is to set the threshold at 4 different points instead of picking just one point. CTS calculates the percentage of the total number of pixels in an image occur on or below each of the pixel intensities.

Another method is segmentation and skeletonization of digital images. Morrison and Young developed a technique to quantify microglia morphology by skeletonization of digital images (Young & Morrison, 2018). On the other hand, we can manual or semiautomatic tracing and reconstruction of immunolabeled cells. All these approaches need to satisfactorily handle difficulties for consistency and reliability of the data, high quality histological processing, and microscopy. The main issue with single cell reconstructions is when cell processes are not entirely contained in the reconstruction, or when supervised or unsupervised tracing erroneously assigns processes to a given cell. We choose to use semiautomatic tracing to reduce erroneously assigned processes to a given cell. Once we get a reconstruction, we can use Sholl analysis to analysis the number of intersections and nodes of the microglia to determine its “bushiness”.

Three-dimensional (3D) reconstruction is a method to obtain Sholl analysis metrics including intersections, nodes, total length, surface area, volume, and average diameter. Together these metrics can quantitatively measure the "bushiness" of the microglia. An advantage of 3D reconstructions is that we can focus on a single cell rather than a region. However, disadvantages of 3D reconstructions are that the method requires specialty software, no currently standard method, and that it is time-consuming. This is an ongoing challenge in the field of neuroscience as new techniques are being developed.

An issue with Sholl analysis is that experiments usually sample multiple microglia per animal which are then analyzed using simple linear models. These models fail to account for intra-class correlation that occurs with clustered data which can lead to faulty inferences. One of the solutions of this issue is to use mixed effects models. Another method is to average the measurements across microglia to obtain one observation per animal at each radius, then use repeated measures analysis across radii. This approach does not violate any model assumptions, but it does result in a loss of information about variability across the microglia. (Wilson et al, 2017) Since microglia are heterogenous, the loss of variability across microglia is important, because not all microglia are reacting in the same way.

Conclusion:

Microglia respond to peripheral allergic inflammation in a sex-dependent manner in the hippocampus. At baseline in the adult microglia, sex differences in microglia density are present and in response to Alternaria exposure, females are more reactive than males, increasing their cell density and increasing their surveillance capacity. Sex differences in microglia response could have implications in sex differences in neurological diseases. Future experiments should consider sex as a biological variable and sex differences in their data sets.

References:

2021 Alzheimer's disease facts and figures. (2021). *Alzheimer's and Dementia*, *17*(3), 327–406. https://doi.org/10.1002/alz.12328

Ardekani, B. A., Convit, A., & Bachman, A. H. (2016). Analysis of the MIRIAD Data Shows Sex Differences in Hippocampal Atrophy Progression. *Journal of Alzheimer's Disease : JAD*, *50*(3), 847–857. https://doi.org/10.3233/JAD-150780

Bachstetter, A. D., van Eldik, L. J., Schmitt, F. A., Neltner, J. H., Ighodaro, E. T., Webster, S. J., Patel, E., Abner, E. L., Kryscio, R. J., & Nelson, P. T. (2015). Disease-related microglia heterogeneity in the hippocampus of Alzheimer's disease, dementia with Lewy bodies, and hippocampal sclerosis of aging. *Acta Neuropathologica Communications*, *3*, 32. https://doi.org/10.1186/S40478-015-0209-Z

Bonham, L. W., Sirkis, D. W., & Yokoyama, J. S. (2019). The Transcriptional Landscape of Microglial Genes in Aging and Neurodegenerative Disease. *Frontiers in Immunology*, *10*(JUN). https://doi.org/10.3389/FIMMU.2019.01170

Carson, M. J. (2012). Molecular Mechanisms and Consequences of Immune and Nervous System Interactions. *Basic Neurochemistry*, 597. https://doi.org/10.1016/B978-0-12-374947-5.00033-X

Carson, M. J., Doose, J. M., Melchior, B., Schmid, C. D., & Ploix, C. C. (2006). CNS immune privilege: hiding in plain sight. In *Immunological Reviews* (Vol. 213).

Davalos, D., Grutzendler, J., Yang, G., Kim, J. v., Zuo, Y., Jung, S., Littman, D. R., Dustin, M. L., & Gan, W. B. (2005). ATP mediates rapid microglial response to local brain injury in vivo. *Nature Neuroscience*, *8*(6), 752–758. https://doi.org/10.1038/nn1472

Ewald, A. C., Kiernan, E. A., Roopra, A. S., Radcliff, A. B., Timko, R. R., Baker, T. L., & Watters, J. J. (2020). Sex- And region-specific differences in the transcriptomes of rat microglia from the brainstem and cervical spinal cord. *Journal of Pharmacology and Experimental Therapeutics*, *375*(1), 210–222. https://doi.org/10.1124/JPET.120.266171

Franco-Bocanegra, D. K., Gourari, Y., McAuley, C., Chatelet, D. S., Johnston, D. A., Nicoll, J. A. R., & Boche, D. (2021). Microglial morphology in Alzheimer's disease and after Aβ immunotherapy. *Scientific Reports 2021 11:1*, *11*(1), 1–12. https://doi.org/10.1038/s41598-021-95535-0

Ginhoux, F., Greter, M., Leboeuf, M., Nandi, S., See, P., Gokhan, S., Mehler, M. F., Conway, S. J., Guan Ng, L., Richard Stanley, E., Samokhvalov, I. M., & Merad, M. (2009). Supporting Online Material Fate Mapping Analysis Reveals That Adult Microglia Derive from Primitive Macrophages. *Proc. Natl. Acad. Sci. U.S.A*, *136*, 1168. https://doi.org/10.1126/science.1194554

Guneykaya, D., Ivanov, A., Hernandez, D. P., Haage, V., Wojtas, B., Meyer, N., Maricos, M., Jordan, P., Buonfiglioli, A., Gielniewski, B., Ochocka, N., Cömert, C., Friedrich, C., Artiles, L. S., Kaminska, B., Mertins, P., Beule, D., Kettenmann, H., & Wolf, S. A. (2018). Transcriptional and Translational Differences of Microglia from Male and Female Brains. *Cell Reports*, *24*(10), 2773-2783.e6. https://doi.org/10.1016/j.celrep.2018.08.001

Hammond, T. R., Dufort, C., Dissing-Olesen, L., Giera, S., Young, A., Wysoker, A., Walker, A. J., Gergits, F., Segel, M., Nemesh, J., Marsh, S. E., Saunders, A., Macosko, E., Ginhoux, F., Chen, J., Franklin, R. J. M., Piao, X., McCarroll, S. A., & Stevens, B. (2019a). Single-Cell RNA Sequencing of Microglia throughout the Mouse Lifespan and in the Injured Brain Reveals Complex Cell-State Changes. *Immunity*, *50*(1), 253-271.e6. https://doi.org/10.1016/j.immuni.2018.11.004

Hammond, T. R., Dufort, C., Dissing-Olesen, L., Giera, S., Young, A., Wysoker, A., Walker, A. J., Gergits, F., Segel, M., Nemesh, J., Marsh, S. E., Saunders, A., Macosko, E., Ginhoux, F., Chen, J., Franklin, R. J. M., Piao, X., McCarroll, S. A., & Stevens, B. (2019b). Single-Cell RNA Sequencing of Microglia throughout the Mouse Lifespan and in the Injured Brain Reveals Complex Cell-State Changes. *Immunity*, *50*(1), 253-271.e6. https://doi.org/10.1016/j.immuni.2018.11.004

Johnson, S. J., & Walker, F. R. (2015). Strategies to improve quantitative assessment of immunohistochemical and immunofluorescent labelling. *Scientific Reports 2015 5:1*, *5*(1), 1–4. https://doi.org/10.1038/srep10607

Klein, B., Mrowetz, H., Thalhamer, J., Scheiblhofer, S., Weiss, R., & Aigner, L. (2016). Allergy Enhances Neurogenesis and Modulates Microglial Activation in the Hippocampus. *Frontiers in Cellular Neuroscience*, *10*(Jun). https://doi.org/10.3389/FNCEL.2016.00169

Kongsui, R., Beynon, S. B., Johnson, S. J., & Walker, F. R. (2014). Quantitative assessment of microglial morphology and density reveals remarkable consistency in the distribution and morphology of cells within the healthy prefrontal cortex of the rat. *Journal of Neuroinflammation*, *11*(1). https://doi.org/10.1186/s12974-014-0182-7

Lawson, L. J., Perry, V. H., Dri, P., & Gordon, S. (1990). Heterogeneity in the distribution and morphology of microglia in the normal adult mouse brain. *Neuroscience*, *39*(1), 151–170. https://doi.org/10.1016/0306-4522(90)90229-W

Li, Q., Cheng, Z., Zhou, L., Darmanis, S., Neff, N. F., Okamoto, J., Gulati, G., Bennett, M. L., Sun, L. O., Clarke, L. E., Marschallinger, J., Yu, G., Quake, S. R., Wyss-Coray, T., & Barres, B. A. (2019). Developmental Heterogeneity of Microglia and Brain Myeloid Cells Revealed by Deep Single-Cell RNA Sequencing. *Neuron*, *101*(2), 207-223.e10. https://doi.org/10.1016/j.neuron.2018.12.006

Liu, Y. U., Ying, Y., Li, Y., Eyo, U. B., Chen, T., Zheng, J., Umpierre, A. D., Zhu, J., Bosco, D. B., Dong, H., & Wu, L. J. (2019). Neuronal network activity controls microglial process surveillance in awake mice via norepinephrine signaling. *Nature Neuroscience*, *22*(11), 1771. https://doi.org/10.1038/S41593-019-0511-3

Masuda, T., Sankowski, R., Staszewski, O., & Prinz, M. (2020). Microglia Heterogeneity in the Single-Cell Era. In *Cell Reports* (Vol. 30, Issue 5, pp. 1271–1281). Elsevier B.V. https://doi.org/10.1016/j.celrep.2020.01.010

Mizutani, M., Pino, P. A., Saederup, N., Charo, I. F., Ransohoff, R. M., & Cardona, A. E. (2012). The fractalkine receptor but not CCR2 is present on microglia from embryonic development throughout adulthood. *Journal of Immunology (Baltimore, Md. : 1950)*, *188*(1), 29–36. https://doi.org/10.4049/JIMMUNOL.1100421

Morgan, J. T., Chana, G., Pardo, C. A., Achim, C., Semendeferi, K., Buckwalter, J., Courchesne, E., & Everall, I. P. (2010). Microglial Activation and Increased Microglial Density Observed in the Dorsolateral Prefrontal Cortex in Autism. *Biological Psychiatry*, *68*(4), 368–376. https://doi.org/10.1016/J.BIOPSYCH.2010.05.024

Nimmerjahn, A., Kirchhoff, F., & Helmchen, F. (2004). 14. See supporting data on Science. *Proc. Natl. Acad. Sci. U.S.A*, *38*, 286. https://doi.org/10.1126/science.1107891

Okeke, C. C. (2021). *Quantifying Changes to the 3D Structure of Microglia in Response to an Insult from Inhalation of Alternaria Alternata Particulate Matter*. UC Riverside.

Peng, X., Madany, A. M., Jang, J. C., Valdez, J. M., Rivas, Z., Burr, A. C., Grinberg, Y. Y., Nordgren, T. M., Nair, M. G., Cocker, D., Carson, M. J., & Lo, D. D. (2018). Continuous Inhalation Exposure to Fungal Allergen Particulates Induces Lung Inflammation While Reducing Innate Immune Molecule Expression in the Brainstem. *ASN Neuro*, *10*. https://doi.org/10.1177/1759091418782304

Qin, L., Wu, X., Block, M. L., Liu, Y., Breese, G. R., Hong, J.-S., Knapp, D. J., & Crews, F. T. (2007). *Systemic LPS Causes Chronic Neuroinflammation and Progressive Neurodegeneration NIH Public Access*. *55*(5), 453–462. https://doi.org/10.1002/glia.20467

Schwarz, J. M., Sholar, P. W., & Bilbo, S. D. (2012). Sex differences in microglial colonization of the developing rat brain. *Journal of Neurochemistry*, *120*(6), 948. https://doi.org/10.1111/J.1471-4159.2011.07630.X

Smolders, S. M. T., Kessels, S., Vangansewinkel, T., Rigo, J. M., Legendre, P., & Brône, B. (2019). Microglia: Brain cells on the move. In *Progress in Neurobiology* (Vol. 178). Elsevier Ltd. https://doi.org/10.1016/j.pneurobio.2019.04.001

Ulrich, J. D., Ulland, T. K., Colonna, M., & Holtzman, D. M. (2017). Elucidating the Role of TREM2 in Alzheimer's Disease. *Neuron*, *94*(2), 237–248. https://doi.org/10.1016/J.NEURON.2017.02.042

Valdez, J. M. (2021). *Systemic Inflammation Affects the CNS in an Age, Duration, and Sex Dependent Manner* [UCR Riverside]. https://escholarship.org/uc/item/72d9f91x

Villa, A., Gelosa, P., Castiglioni, L., Cimino, M., Rizzi, N., Pepe, G., Lolli, F., Marcello, E., Sironi, L., Vegeto, E., & Maggi, A. (2018). Sex-Specific Features of Microglia from Adult Mice. *Cell Reports*, *23*(12), 3501–3511. https://doi.org/10.1016/j.celrep.2018.05.048

Wake, H., Moorhouse, A. J., Jinno, S., Kohsaka, S., & Nabekura, J. (2009). Resting microglia directly monitor the functional state of synapses in vivo and determine the fate of ischemic terminals. *Journal of Neuroscience*, *29*(13), 3974–3980. https://doi.org/10.1523/JNEUROSCI.4363-08.2009

Young, K., & Morrison, H. (2018). Quantifying Microglia Morphology from Photomicrographs of Immunohistochemistry Prepared Tissue Using ImageJ. *J. Vis. Exp*, *136*, 57648. https://doi.org/10.3791/57648